

Investigation of Material Property Model on Substrate Deformation Induced by Thick-Walled WAAM Process Using Numerical Computation



Siti Nursyahirah Ahmad , Yupiter Harangan Prasada Manurung ,
Muhd Faiz Mat , and Martin Leitner 

Abstract This research presents an investigation of material property model effects of thick-walled Wire Arc Additive Manufacturing (WAAM) process on deformation behaviour which involves thermo-mechanical non-linear numerical computation. A 3D thermo-elastic-plastic WAAM model is developed using general purposed FEA software MSC Marc/Mentat. The material models of component stainless steel SS316L were simulated based on two different sources namely material X5CrNiMo18_10_1 from default library database and evolved wire. The thermo-mechanical and thermo-physical material properties of evolved wire SS316L were obtained using chemical composition analysis SEDM-EDX and generated by advanced material modelling software. Component geometry was modelled using simplified rectangular shape and mesh which consists of ten layers and three strings. The numerical simulation was implemented under consideration of temperature dependent hardening rule with von-mises yield criteria and Goldak's double ellipsoid heat source model was utilized. Based on the adjusted thermal coefficient parameters, the transient temperature distribution between two different material property models were analysed. The outcome of this research is to characterise the substrate deformation induced by WAAM process using material models of evolved component SS316L and existing material from default library database.

Keywords WAAM · Material modelling · SS316L · Numerical computation · Deformation

S. N. Ahmad · Y. H. P. Manurung (✉) · M. F. Mat
Smart Manufacturing Research Institute (SMRI), Universiti Teknologi MARA (UiTM), Shah Alam, Selangor, Malaysia
e-mail: yupiter.manurung@uitm.edu.my

M. F. Mat · M. Leitner
Chair of Mechanical Engineering, Montanuniversität Leoben, Leoben, Austria

1 Introduction

Additive manufacturing processes (AM) are one of the most essential innovations in the manufacturing sector for the production of metal components. Nowadays, AM is extensively used in the manufacture of build-up products by layer deposition instead of traditional raw material machining. In fact, these technologies offer several advantages, such as the possibility of manufacturing parts with complex geometries and a substantial reduction of material waste in machining processes. A fundamental AM system comprises a combination of a heat source, motion system, and feedstock. In addition, AM is a promising alternative for manufacturing parts or components made of high-end materials such as titanium or aluminum alloys due to the high degree of the buy-to-fly ratio. Hence, metallic additive manufacturing processes are subdivided into three different categories which are powder-feed, powder-bed, and wire-feed systems [1].

Many techniques for the manufacture of metal structures in AM have been developed, one of promising breakthrough for AM technology is Wire Arc Additive Manufacturing (WAAM) have been gaining enormously in popularity for decades in the metallic parts with complex structure and geometry [1]. Among metal AM processes, WAAM process also accomplished by employing a layer- by- layer strategy that can create a large part with a higher deposition rate [2]. WAAM is made up of a combination of electric arc heating sources with a metallic wire feeding system in which the building strategy allows the production of metal components layer by layer by means of Gas Metal Arc Welding (GMAW) technology. A component manufactured by a wire-based additive manufacturing method can achieve the tensile strength of casting or forging complex component [3]. The filler material is usually melted by means of an electric arc between the consumable wire feedstock and the top surface of the deposited layers, while the deposit-formed component experiences heating and cooling with the moving heat source model [4].

However, due to the poor surface finish and low accuracy in comparison with powder-bed or beam-melting additive technologies, it is important to determine the interaction of each assigned process parameter with the material properties such as chemical composition for producing high quality product. An initial prediction can be made using numerical computation taking thermal–mechanical properties and different boundary conditions into consideration [5, 6]. From a numerical simulation perspective, WAAM process is very similar to multi-pass welding process. The numerical computation of WAAM process carries out the similar techniques applied in the multi-passes welding simulation due to phenomenon of heat transfer from the arc to the molten pool of work piece. Thus, the heat propagation in GMAW-based additive manufacturing is highly non-linear due to the existence of solidification, multiple fusion and phase transformation [7].

The multi-layered WAAM process is usually simulated based on coupled thermo-mechanical FEM analysis. Ding et al. has performed a research of optimization of thermo-elastic–plastic FEM model of WAAM process on large multi-layered parts and reported that FEM approach introduced can provide an accurate prediction of

the distortion within short computational time [8]. Besides, the heat transfer from the arc to the molten pool is simulated using a heat source model, which prescribes a heat generation per unit volume in the molten pool region. In most of literature works dealing with AM simulation, the heat source model proposed by Goldak et al. is applied [9]. In this model, the heat input is delivered over a moving double ellipsoid region according to a Gaussian distribution. Despite such strategy permits to correctly model the shape of the weld pool, it does not consider the correct heat distribution between filler and base material. This is responsible for inaccuracies in part distortions estimation.

In this research, an efficient FEM procedure is to be developed with a series of experiment of thick-walled WAAM structure with ten layers and three strings in order to analyse the thermo-mechanical behaviour. A numerical computation is carried out using two different material models which are namely existing material of numerical simulation database and evolved material model of stainless steel SS36L obtained from experiment. Further, a comparison between these two material modelling strategies will be observed on substrate deformation and transient temperature distribution.

2 Non-linear Numerical Simulation for WAAM Process

In order to analyse the therm-mechanical behaviour of the WAAM structure, the general purposed FEM software MSC Marc/Mentat was utilized to perform coupled thermo-mechanical numerical simulation which requires the modelling of geometry, material and heat source.

2.1 Geometrical Modelling of Thick-Walled WAAM Simulation

A 3D-solid FE model of thick-walled WAAM component was developed consisting three sets of geometries as shown in Fig. 1 namely a table, a base plate and multi-layers WAAM beads. The base plate was modelled with dimension of 200 mm (L) \times 97.5 mm (W) \times 8 mm (T). Multi-layered deposited walls with a rectangular-shaped weld bead of 150 mm length was modelled with three strings and ten layers. The work piece is meshed by Herrmann Formulation eight node brick elements types. The WAAM model consists of 14,892 nodes with the table, plate and weld beads are divided into 180 element, 6000 elements, and 5400 elements respectively.

In this research, the bead modelling strategy utilizes simpler rectangular shape which can reduce unnecessary pre-processing effort and allow shorter computational time. Hence, 'element birth technique' was applied to model the filler material. All

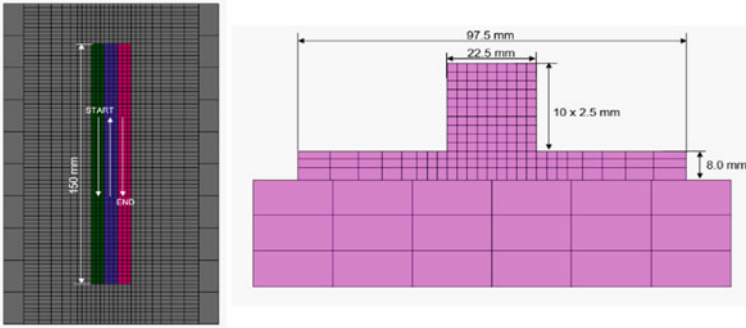
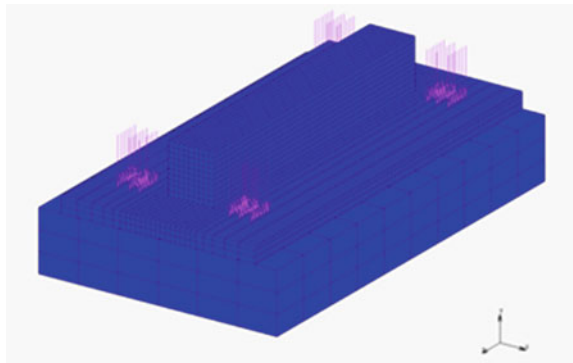


Fig. 1 Direction and geometrical model of WAAM

elements of weld bead are deactivated at the initial status of analysis and then activated sequentially following the heat source movements [10–12].

As mechanical boundary conditions, four clamps were exerted on the top surfaces of the plates and the holding force of clamps were set equal to 400 N. Figure 2 presents the clamping force on the base plate in negatively Y-directions. The change in the temperature distribution contributes to the deformation of the body through thermal strains and influences the material properties. In addition, phase transformation effect is not considered in the numerical analysis. The modelling of the fluid flow is also not included because the effect of the fluid flow on the deformation and stress field can be considered as negligible [13].

Fig. 2 The boundary conditions with industrial clamping locations



2.2 Material Modelling and Properties Evolution of Component SS316L

For characterising the temperature-dependent material properties, the experimental determination of the evolved microstructure is measured under consideration of the adjusted microstructure from the real process. The analysis of thermo-mechanical and thermo-physical properties of the filler material was performed. The actual filler material used in the WAAM process possess chemical composition was determined by the SEM-EDX machine Hi-Tech Instrument SU3500 as presented in Fig. 3. The measured analysis lays in the range of the relevant standard of the filler material SS316L.

Table 1 shows the results of characterization. Based on this chemical composition, new material properties will be generated using advanced material modelling software.

The major temperature-dependent properties (Fig. 4) such as the specific heat capacity, heat conductivity coefficient, thermal expansion coefficient and Young's modulus are calculated based on the chemical composition analysis as obtained from Table 1 using material modelling software. These data were then implemented into FEM software MSC Marc/Mentat for further calculation.

Fig. 3 Chemical composition analysis using SEM-EDX machine hi tech instrument SU3500



Table 1 The actual chemical composition of filler material SS316L

Material	C	Cu	Cr	Mn	Mo	Ni	Si	Ti	V
Evolved SS316L	0.03	0.76	17.83	2.43	1.63	10.57	0.63	0.267	0.3

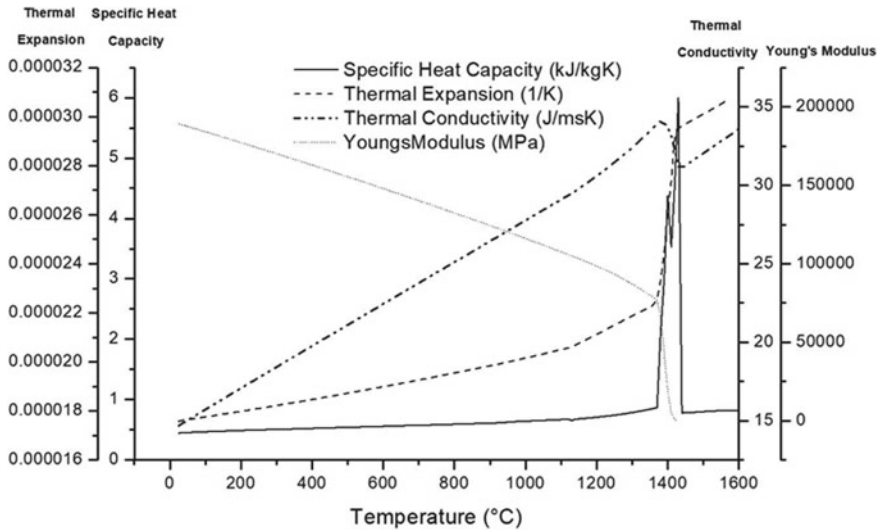


Fig. 4 Thermo-mechanical properties of evolved component SS316L

In this study, the numerical computation of thick-walled WAAM process is also executed using the existing databases from the MSC Marc/Mentat of material properties library. The thermo-physical material properties of material databases of X5Crnimo18_10_1 are predicted equivalent with the austenitic stainless steel SS316L. Figure 5 shows the material X5Crnimo18_10_1 assigned for the WAAM model with temperature-dependent variables. The effect on the substrate deformation of thick-walled WAAM using two different material properties will be analysed and compared.

In the following simulation, a low carbon steel S235 is designated as substrate material of thick-walled WAAM. Both thermo-physical material properties are imported into FEM simulation. Figure 6 shows the material S235 assigned for the FE model with temperature-dependent variables.

2.3 Numerical Computation Parameters and Heat Source Modelling

In this simulation, WAAM parameters which are implemented on the MSC Marc/Mentat as displayed in Table 2. Therefore, the Current (I) and the Voltage (V) are considered under power equation. The assigned travel speed (v) was based on the experimental welding speed for this material in order to develop a more realistic model.

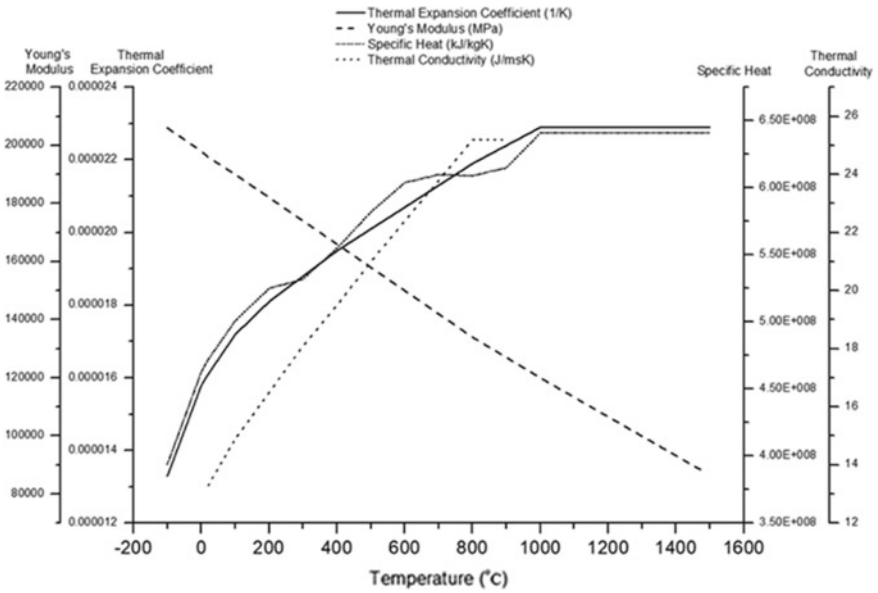


Fig. 5 Temperature-dependent thermo-mechanical and thermo physical properties X5CrNiMo18_10_1

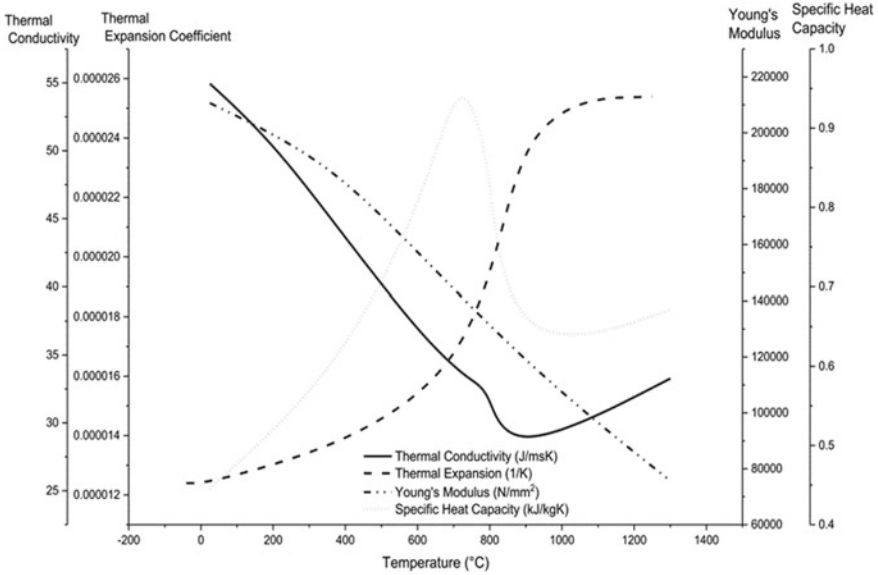
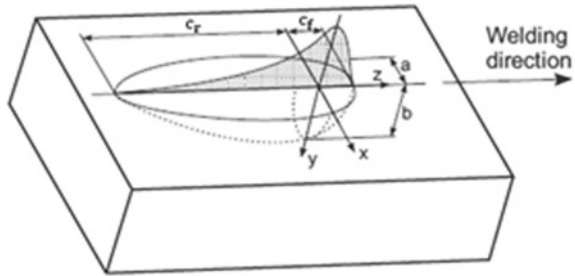


Fig. 6 Temperature-dependent of material properties S235

Table 2 WAAM parameters used in MSC marc mentat

WAAM parameters	Value
Current, I (A)	172
Voltage, V (V)	19.8
Travel Speed, v (mm/s)	5
Efficiency, η	0.8

Fig. 7 Model of the double ellipsoid heat source by Goldak



One of the challenges in the numerical simulation of WAAM process is the modelling of the heat source. Suitable heat source model must be chosen in accordance with the WAAM process. Hence, for GMAW process, Goldak’s double ellipsoid model was executed to replicate the real heat source. This model is a widely used heat source model for GMAW process, which has been shown to accurately represent the heat power density from an electric arc traversing across the surface of a flat plate [14–16]. Figure 7 presents Goldak’s double ellipsoid heat source model with the geometrical conditions. The geometrical parameters a, b and c can be modified in values for the front or rear quadrants.

The subsequent equations were used to characterize the power density distribution inside the front and rear quadrants of the heat source along the welding path (z-axis). The power density of the heat flux in front section (q_{vf}) of heat source can be modelled with Eq. (1) and the rear section (q_{vr}) with Eq. (2).

$$q_{vf}(x, y, z) = \frac{6\sqrt{3}f_f Q}{abc_f \pi \sqrt{\pi}} e^{-3\frac{x^2}{a^2}} . e^{-3\frac{y^2}{b^2}} . e^{-3\frac{z^2}{a_f^2}} \tag{1}$$

$$q_{vr}(x, y, z) = \frac{6\sqrt{3}f_r Q}{abc_r \pi \sqrt{\pi}} e^{-3\frac{x^2}{a^2}} . e^{-3\frac{y^2}{b^2}} . e^{-3\frac{z^2}{a_r^2}} \tag{2}$$

The distribution of heat fluxes in the double ellipsoid model is determined by four directions: width (a), depth (b), rear length (c_r) and front length (c_f), whereas c_r and c_f are the heat deposited fractional factors in the rear and front quadrant respectively and the sum is equal to two [17, 18]. Detailed values for each direction are shown in Table 3. Figure 8 illustrates the heat distribution of heat source model of Goldak’s double ellipsoid.

Table 3 Goldak’s double ellipsoidal heat source dimension in FEM simulation

Heat source dimensions (mm)	Value
Width	7.5
Depth	3
Rear length, c_r	5
Front length, c_f	12

Fig. 8 The heat distribution induced by Goldak’s double ellipsoid model with the respect heat source size dimensions

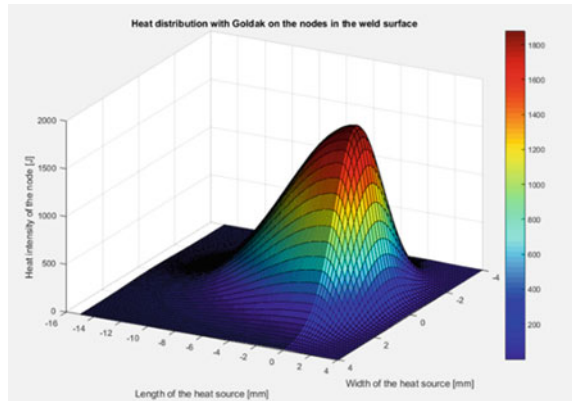


Table 4 Calibrated numerical boundary conditions on thick-walled WAAM model

Numerical parameters	Value
Heat transfer coefficient, metal to metal ($W/m^2/K$)	2500
Heat transfer coefficient, metal to environment ($W/m^2/K$)	25
Initial temperature ($^{\circ}C$)	25

In this WAAM simulation, the thermal material properties of evolved component SS316L which are latent heat ($2.56e+11 \text{ mm/s}^2$), solidus temperature ($1279 \text{ }^{\circ}C$) and liquidus temperature ($1450 \text{ }^{\circ}C$). Table 4 summarizes the adjusted thermal boundary conditions implemented in the numerical computation.

3 Result and Discussions

Figure 9 shows a comparison of transient temperature distribution between filler material of evolved feedstock SS316L and X5Crnimo18_10_1 depicting the thermal cycles of the testing point in the weld zone of first string of first layer. The peak temperature of evolved component SS316L and X5Crnimo18_10_1 has reached about $1170 \text{ }^{\circ}C$ and $1060 \text{ }^{\circ}C$ respectively.

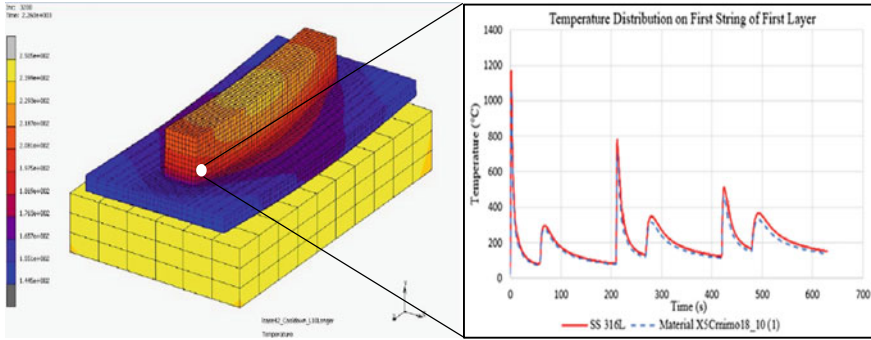


Fig. 9 Comparison of thermal histories between evolved SS316L components and Material X5Crni18_10_1

Figure 10 demonstrates the moving heat source of WAAM model with different material properties of component. It can be observed that isothermals became narrower when material X5Crni18_10_1 from existing database of library are used. It leads to larger temperature gradient directly affecting the cooling rates as well as substrate deformations.

The substrate deformation analysis is conducted between these two feedstocks. Figure 11 exhibits a contour band model from numerical simulation software MSC Marc/Mentat which displays the displacement result of numerical computation of thick-walled WAAM model in y-direction.

The substrate deformation analysis can be observed clearly that is presented in Fig. 12. It shows that the substrate deformation induced by evolved feedstock SS316L

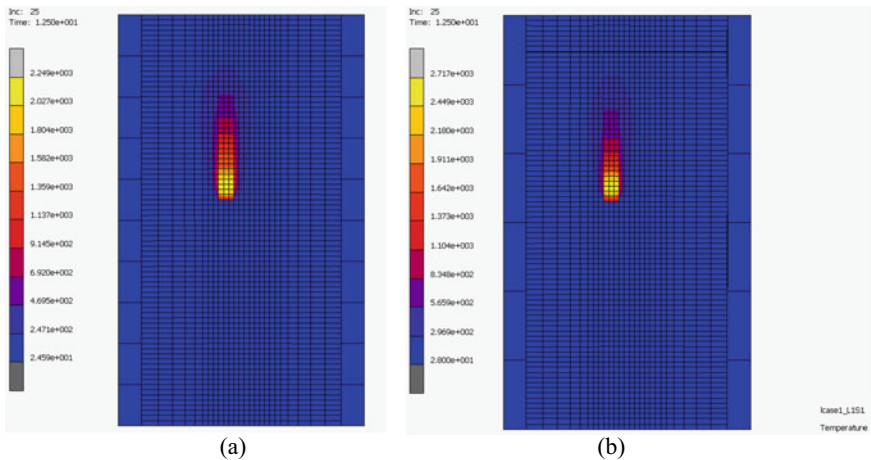


Fig. 10 The heat distribution of WAAM model by using material properties of weld bead **a** Evolved SS316L and **b** X5Crni18_10_1

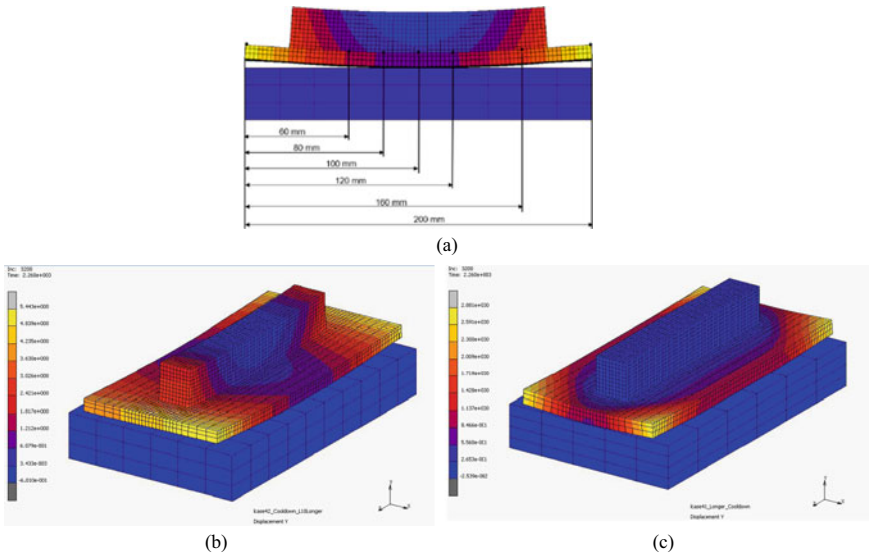


Fig. 11 The substrate deformation induced by WAAM process **a** distortion measurement, **b** evolved component SS316L and **c** material X5CrNiMo18_10_1

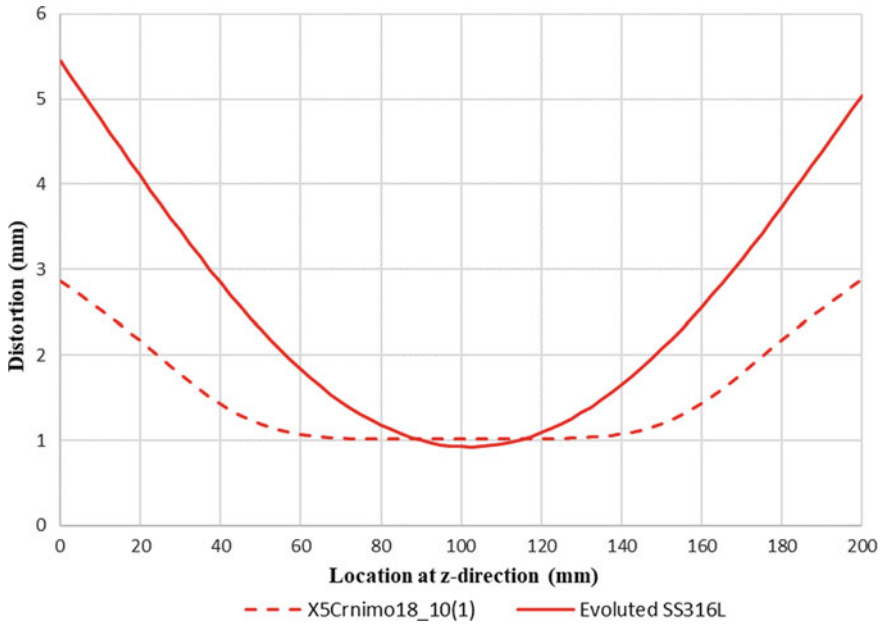


Fig. 12 Substrate distortion along z-direction on the length of the substrate

is higher than feedstock material X5Crnimo18_10_1. According to this result, it shows that the nonlinear temperature-dependent of material properties of the feedstock has a significant effect on the transient temperature and substrate deformation of WAAM process. Table 5 shows the substrate deformation results of thick-walled WAAM model.

4 Conclusion

In this research, an investigation focusing on deformation of substrate material and thermal history were conducted based on the effect of property material modelling of WAAM process using numerical simulation. All the parameters, geometrical modelling and boundary conditions are developed in the similar manner. By using different material modelling approaches, the transient thermal distribution as well as substrate deformation on a thick-walled WAAM component were compared between two different material modelling approaches. According to the results in this study, it can be summarized that the numerical computational analysis for ten layers with three strings of thick-walled WAAM component has been successfully executed with the structured procedure. The nonlinear temperature-dependent mechanical and physical properties of evolved feedstock SS316L were determined experimentally as well as calculated using material modelling software, which predict the material behaviour under consideration of the chemical composition analysis.

Based on the results, the thermal cycles and higher heating and cooling rates are developed during WAAM process which gives significant effect on substrate deformation. By comparing the WAAM simulation, the model which utilises existing database library X5Crnimo18_10 (1) material has higher relative percentage errors with 29% compared to the numerical simulation of WAAM model using evolved feedstock SS316L. The deviation of temperature distribution and substrate distortion result between these two feedstock materials are caused by the material properties implemented within each WAAM model as well as different plasticity models based on an isotropic hardening rule of flow curves.

As further recommendation, an advanced investigation can be executed on substrate deformation analysis and thermal calibration of austenitic stainless steel of SS316L using numerical simulation and experimental verification. Next, rectangular heat source model will be developed using subroutine algorithm MSC Marc/Mentat.

Table 5 Substrate deformation results of thick-walled WAAM model

Model	Distance (point of measurement) in mm							Average deformation (mm)	Relative percentage errors (%)
	1	2	3	4	5	6	7		
	0	60	80	100	120	160	200		
Evolved SS316L	5.44	1.83	1.18	0.93	1.09	2.56	5.04	2.58	-
X5Cmimo18_10 (1)	2.87	1.07	1.02	1.02	1.02	1.43	2.88	1.62	29.4

Acknowledgements The authors would like to express their gratitude to staff member of Smart Manufacturing Research Institute (SMRI), Research Interest Group: Advanced Manufacturing Technology (RIG:AMT) and Advanced Manufacturing Technology Excellence Centre (AMTEX) at Faculty of Mechanical Engineering, Universiti Teknologi MARA (UiTM) for encouraging this research. This research and conference participation are also financially supported by ASEA-UNINET grant with the project number ASEA 2019/Montan/1, ERASMUS+ (Montan University in Leoben) and Technogerma Engineering and Consulting Sdn. Bhd.

References

1. Wang F, Williams S, Rush M (2011) Morphology investigation on direct current pulsed gas tungsten arc welded additive layer manufactured Ti6Al4V alloy. *Int J Adv Manuf Technol*
2. Brandl E, Baufeld B, Leyens C, Gault R (2010) Additive manufactured Ti-6Al-4V using welding wire: comparison of laser and arc beam deposition and evaluation with respect to aerospace material specifications. *Phys Proc*
3. Hu Z, Qin X, Li Y, Yuan J, Wu Q (2018) Multi-bead overlapping model with varying cross-section profile for robotic GMAW-based additive manufacturing. *J Intell Manuf* 3:2019
4. Xiong J, Li R, Lei Y, Chen H (2018) Heat propagation of circular thin-walled parts fabricated in additive manufacturing using gas metal arc welding. *J Mater Process Technol*
5. Chua BL, Lee HJ, Ahn DG, Kim JG (2018) Influence of process parameters on temperature and residual stress distributions of the deposited part by a Ti-6Al-4V wire feeding type direct energy deposition process. *J Mech Sci Technol* 32(11):5363–5372
6. Wang C, Kim JW (2018) Numerical analysis of distortions by using an incorporated model for welding-heating-cutting processes of a welded lifting lug. *J Mech Sci Technol* 32(12):5855–5862
7. Graf M, Hälsig A, Höfer K (2018) Thermo-mechanical modelling of wire-arc additive manufacturing (WAAM) of semi-finished products
8. Goldak J, Chakravarti A, Bibby M (1984) A new finite element model for welding heat sources. *Metall Trans B*
9. Montevecchi F, Venturini G, Grossi N, Scippa A, Campatelli G (2017) Finite element mesh coarsening for effective distortion prediction in wire arc additive manufacturing. *Addit Manuf* 18:145–155
10. Wang C, Kim YR, Kim JW (2014) Comparison of FE models to predict the welding distortion in T-joint gas metal arc welding process. *Int J Precis Eng Manuf* 15(8):1631–1637
11. Israr R, Buhl J, Elze L, Bambach M (2018) Simulation of different path strategies for wire-arc additive manufacturing with lagrangian finite element methods
12. Goldak JA, Akhlaghi M (2005) Computational welding mechanics
13. Reda R, Magdy M, Rady M (2019) Ti-6Al-4V TIG weld analysis using FEM simulation and experimental characterization. *Iran J Sci Technol Trans Mech Eng* 0123456789
14. Kollár D, Kövesdi B, Vigh LG, Horváth S (2019) Weld process model for simulating metal active gas welding. *Int J Adv Manuf Technol* 102(5–8):2063–2083
15. Darmadi DB, Tieu AK, Norrish J (2012a) A validated thermal model of bead-on-plate welding. *Heat Mass Transf Und Stoffuebertragung* 48(7):1219–1230
16. Velaga SK, Ravisankar A (2017) Finite element based parametric study on the characterization of weld process moving heat source parameters in austenitic stainless steel. *Int J Press Vessel Pip* 157:63–73

17. Darmadi DB, Tieu AK, Norrish J (2012b) A validated thermal model of bead-on-plate welding. *Heat Mass Transf* 48(7):1219–1230
18. GolGdak A, Bibby M (1984) A new finite element model for welding heat sources. *Metall Trans B* 15:299–305